Published in final edited form as:
Neurobiol Dis. 2011 February ; 41(2): 338–352. doi:10.1016/j.nbd.2010.10.002.

Cholinotrophic basal forebrain system alterations in 3xTg-AD transgenic mice

Sylvia E. Perez[a], **Bin He**[a], **Nadeem Muhammad**[a], **Kwang-Jin Oh**[a], **Margaret Fahnestock**[b], **Milos Ikonomovic**[c], and **Elliott J. Mufson**[a]

[a]Department of Neurological Sciences Rush University Medical Center 1735 West Harrison Street, suite 300 Chicago, IL 60612

[b]Department of Psychiatry and Behavioral Neurosciences, McMaster University, 1200 Main Street W Hamilton, ON L8N3Z5 Canada

[c]Departments of Neurology and Psychiatry, University of Pittsburgh School of Medicine, and Geriatric Research Educational and Clinical Center, V.A. Pittsburgh Healthcare System, BSTWR S-521, 200 Lothrop Street Pittsburgh, PA 15213-2536

Abstract

The cholinotrophic system, which is dependent upon nerve growth factor and its receptors for survival, is selectively vulnerable in Alzheimer's disease (AD). But, virtually nothing is known about how this deficit develops in relation to the hallmark lesions of this disease, amyloid plaques and tau containing neurofibrillary tangles. The vast majority of transgenic models of AD used to evaluate the effect of beta amyloid (Aβ) deposition upon the cholinotrophic system over-express the amyloid precursor protein (APP). However, nothing is known about how this system is affected in triple transgenic (3xTg)-AD mice, an AD animal model displaying Aβ plaque- and tangle-like pathology in the cortex and hippocampus, which receive extensive cholinergic innervation. We performed a detailed morphological and biochemical characterization of the cholinotrophic system in young (2-4 months), middle-aged (13-15 months), and old (18-20 months) 3xTg-AD mice. Cholinergic neuritic swellings increased in number and size with age, and were more conspicuous in the hippocampal-subicular complex in aged female than in 3xTg-AD male mice. Stereological analysis revealed a reduction in choline acetyltransferase (ChAT) positive cells in the medial septum/vertical limb of the diagonal band of Broca in aged 3xTg-AD mice. ChAT enzyme activity levels decreased significantly in the hippocampus of middle-aged 3xTg-AD mice compared to age-matched ntg mice. ProNGF protein levels increased in the cortex of aged 3xTg-AD mice, whereas TrkA protein levels were reduced in a gender-dependent manner in aged mutant mice. In contrast, $p75^{NTR}$ protein cortical levels were stable but increased in the hippocampus of aged 3xTg-AD mice. These data demonstrate that cholinotrophic alterations in 3xTg-AD mice are age and gender dependent and more pronounced in the hippocampus, a structure more severely affected with Aβ plaque pathology.

Address correspondence to: Elliott J. Mufson, Ph.D. Professor of Neurological Sciences Alla V. and Solomon Jesmer Chair in Aging Rush University Medical Center 1735 W. Harrison Street Suite 300 Chicago, IL 60612 312-563-3558 tel. 312-563-3571 fax. emufson@rush.edu.
sylvia_e_perez@rush.edu; binhe_2000@yahoo.com; Muhammad_Nadeem@rush.edu; sp8472@gmail.com; emufson@rush.edu
fahnest@mcmaster.ca
ikonomovicmd@upmc.edu

Keywords

Alzheimer's disease; amyloid; cholinergic; nerve growth factor; ChAT; proNGF; $p75^{NTR}$; transgenic mice; TrkA; aging

INTRODUCTION

Alzheimer's disease (AD) is the most common type of dementia among the elderly and is neuropathologically characterized by beta amyloid (Aβ) plaques and neurofibrillary tangles (NFTs) (Arnold et al., 1991). In addition, several neurotransmitter systems are affected including the cholinergic basal forebrain (CBF) projection neurons located within the septal diagonal band and the nucleus basalis of Meynert (Coyle et al., 1983; Mesulam et al., 1983; Whitehouse et al., 1981, 1985), which provide the primary cholinergic innervation to the hippocampus the entire cortical mantle (Mesulam et al., 1983), respectively. During the progression of AD there is atrophy of cholinergic neurons accompanied by a reduction in choline acetyltransferase (ChAT), the synthetic enzyme for the neurotransmitter acetylcholine (ACh), in the cortex and hippocampus (Davies, 1979; Davies and Maloney, 1976; DeKosky et al., 2002; Mufson et al., 1989; Richter et al., 1980), which correlate with cognitive decline and disease severity (DeKosky et al., 1992; Perry et al., 1978; Wilcock et al., 1982).

The differentiation, survival and function of CBF neurons are dependent upon the actions of nerve growth factor (NGF), its high-affinity receptor tyrosine kinase, TrkA (Huang and Reichardt, 2001) and the low affinity pan-neurotrophin receptor $p75^{NTR}$ (Barrett and Bartlett, 1994; Frade and Barde, 1998; Lad et al., 2003). These receptors are produced in CBF neurons and transported to their projection sites (Lad et al., 2003; Sobreviela et al., 1997). Clinical pathological studies suggest that the NGF system shifts from cell survival to cell death during the progression AD (see Mufson et al., 2008). Furthermore, in vitro and in vivo studies indicate that Aβ can interact with TrkA to promote neuronal survival and depending on the physiological state of the organism induce apoptosis via $p75^{NTR}$ (Bulbarelli et al., 2009; Fombonne et al., 2009; Yaar et al., 1997), as well as interact with the α7nAChR nicotinic receptor to disrupt normal cholinergic neurotransmission (Chen et al., 2006; Nagele et al., 2001; Wang et al. 2002), suggesting that Aβ plays a key role in cholinergic dysfunction in AD. Although soluble Aβ oligomers are considered to be neurotoxic, profoundly affecting neural network function (Hartley et al., 1999; Walsh and Selkoe, 2007) and neurotrophic factor expression (Garzon and Fahnestock, 2007), the impact of insoluble Aβ plaque deposition upon the cholinotrophic system remains to be clarified.

Transgenic animals carrying the amyloid precursor protein (APP) and/or presenilin-1 (PS1) familial AD (FAD) gene mutations display forebrain Aβ plaques and cortical and hippocampal cholinotrophic dystrophic neurites (Aucoin et al., 2005; Boncristiano et al., 2002; Buttini et al., 2002; Hernandez et al., 2001; Jaffar et al., 2001; German et al., 2003; Perez et al., 2007; Wong et al., 1999). A mouse model of Down syndrome, which has an increased dosage of the APP gene, displays medial septum cholinergic cell loss/atrophy and a disruption in NGF transport (Cooper et al., 2001; Holtzman et al., 1996; Salehi et al., 2006; Seo and Isacson, 2005). Recently, a triple transgenic mouse (3xTg-AD) harboring the human APP_{Swe}, $PS1_{M146V}$ and Tau_{P301L} gene mutations was developed, which displays both intracellular and extracellular Aβ and tau in an age-dependent manner within the cortex, hippocampus, and amygdala (Mastrangelo and Bowers, 2008; Oddo et al., 2003a,b; Oh et al., 2010) and to a lesser degree, in the brainstem (Overk et al., 2009). However, whether the cholinotrophic system in these mice is altered is not known. Therefore, we

performed a detailed morphologic and biochemical evaluation of the cholinotrophic system in young (2-4 months), middle-aged (13-15 months), and old (18-20 months) homozygous 3xTg-AD relative to age-matched non-transgenic (ntg) mice.

MATERIALS AND METHODS

Transgenic mice and tissue preparation

A total of 147 mice (both genders) consisting of homozygous 3xTg-AD mice harboring three human mutant genes: amyloid precursor protein (APP_{Swe}), presenilin-1 ($PS1_{M146V}$) and tau (tau_{P301L}) or age-matched non-transgenic (ntg) mice were used for biochemical (n=75) and histological (n=72) analysis. Both the APP_{Swe} and tau_{P301L} transgenes are co-integrated at the same locus and expressed under control of the mouse Thy1.2 promoter in homozygous $PS1_{M146V}$ (knock-in) mice (Oddo et al., 2003b). All animals were derived from breeding pairs provided by Dr. F. LaFerla (UC Irvine, Irvine, CA) and were housed in our breeding colony (Oh et al., 2010; Overk et al., 2009). Mice were divided into three groups: young (2-4 months), middle-aged (13-15 months) and old (18-20 months). Animal care and procedures were conducted according to the National Institutes of Health Guide for the Care and Use of Laboratory Animals.

Mice were anesthetized with ketamine/xylazine (85mg/kg/9.5mg/kg, i.p.) and transcardially perfused with ice-cold 0.9% sodium chloride solution. For biochemical analysis (ChAT radioenzymatic assay and quantitative immunoblotting), 11 (5 female, 6 male) 2 to 3 month-old, 13 (7 female, 6 male) 13 to 15 month-old and 13 (6 female, 7 male) 18 to 20 month-old 3xTg-AD mice and age-matched ntg mice (n=37) were examined. Brains were rapidly removed from the calvarium and sectioned into 1 mm coronal slabs on wet ice in a stainless steel brain blocker. We cut each brain into 1 mm slabs in order to collect both superficial and deep forebrain structures. Hippocampal-subicular complex tissue was dissected from slabs extending from Bregma −1.06 mm to −4.36 mm, whereas cortical samples were harvested from Bregma 3.20 to −4,60 according to the mouse atlas of Paxinos and Franklin (2001). These individual samples were frozen at −80°C until prior to use for bioassay analysis. All tissue from one hemisphere was used for the determination of ChAT enzyme activity, whereas tissue from the other side was processed for quantitative immunoblotting. Hippocampal-subicular complex tissue from each slab/per hemisphere/per case was combined for bioassay determinations. For immunohistochemistry, 6 male and 6 female 3xTg-AD mice at ages 2-4, 13-15 and 18-20 months and age-matched ntg mice were transcardially perfused with 4% paraformaldehyde and 0.1% glutaraldehyde in 0.1 M phosphate buffer and post-fixed in the same fixative for 12 hours at 4°C. Brains were cryoprotected in 30% sucrose at 4°C until the brain sank and cut on a freezing sliding knife microtome in the coronal plane at a thickness of 40 μm.

Immunohistochemistry

Free-floating sections were single and/or double stained with antibodies against ChAT (1:1000, Millipore, Bedford, MA) and Aβ/APP (6E10; 1:2000, Covance, Princeton, NJ) and the tau conformational antibody Alz50 (~66kDa; 1:10,000), a gift from Dr. Peter Davies, (Albert Einstein School of Medicine, NY) and the phosphoepitope tau antibody AT8 (~66 kDa; 1:1000, Thermofisher, Waltham, MA) for immunohistological and stereological neuron counts as previously described (Perez et al., 2007; Oh et al., 2010; Overk et al., 2009). For single ChAT immunostaining and stereology, sections were incubated in goat anti-human ChAT for 48 hours in a solution containing 1% Triton X-100 and 1% normal horse serum in Tris-buffered saline (TBS) to facilitate penetration of the antibody throughout the full depth of the tissue. Sections were then incubated with biotinylated horse anti-goat secondary antibodies (1:200, Vector Laboratories, Burlingame, CA) for 1 hour.

Subsequently, the reaction was developed in an acetate-imidazole buffer containing 0.05% 3,3′-diaminobenzidine tetrahydrochochloride (DAB, Sigma, St. Louis, MO) and 0.0015% H_2O_2. The reaction was terminated using the acetate-imidazole buffer solution. Sections were mounted on glass slides, dehydrated in graded alcohols, cleared in xylenes and coverslipped with DPX (Biochemica Fluka, Buchs, Switzerland). Sections from all experimental groups were processed at the same time using the same chemical reagents to avoid batch-to-batch variation during immunostaining. Additional sections were dual-labeled for ChAT and Aβ/APP. For double immunostaining, ChAT was developed using nickel intensification as a chromagen (Perez et al., 2005) followed by incubation with the monoclonal 6E10 antibody and visualized using DAB only, as described above. This dual staining method results in a two-colored profile: blue/black ChAT-positive profiles and brown Aβ/APP-containing neurons and plaques. Alz50 or AT8 single and dual immunostaining with ChAT was similar to that described here and in a previous paper (Oh et al., 2010). In addition, several sections from 13-15 and 18-20 month-old 3xTg-AD mice groups were double stained with the 6E10 antibody and for thioflavine-S and cover slipped in an aqueous mounting medium (Biomeda Corp, Foster City, CA) as previously described (Perez et al., 2007). The dual immunofluorescence staining was visualized with the aid of a Zeiss Fluorescent Microscope. Specificity of the ChAT, 6E10, Alz50 and AT8 antibodies was previously described (Mesulam et al., 1983; Oh et al., 2010; Overk et al., 2009). In addition, omission of the primary antibodies resulted in a lack of immunoreactivity.

Stereological analysis

The optical dissector method was used to determine the total number of ChAT-immunoreactive (ChAT-ir) neurons in the medial septum (MS)/vertical limb of the diagonal band of Broca (VDB) in 2 to 4, 13 to 15, and 18 to 20 month-old 3xTg-AD as well as age-matched ntg mice as described previously (Jaffar et al., 2001; Perez et al., 2005, 2007). The region was manually outlined under low magnification and systematically analyzed using a random sampling design. The number of ChAT-ir neurons was estimated using MicroBrightField stereological software (Williston, VT) and a Nikon Optiphot-2 microscope coupled with LEP MAC5000 (BioVision Technologies, Exton, PA, USA). The coefficients of error were calculated according to Gundersen et al. (1988), and values <0.10 were accepted (West, 1993). The thickness of each section was assessed empirically and upper and lower “guard zones” of between 3 and 4 μm were established for each section before measurement. ChAT-ir neurons within MS/VDB were counted from the level of the first appearance of the genu of the corpus callosum to the beginning of the decussation of the anterior commissure (see Fig. 4A-C). An observer blinded to age, gender and genotype performed counts of ChAT positive neurons.

Quantitation of the number and area of cholinergic neurites

To examine the effect of age upon cortical and hippocampal ChAT-ir dystrophic neurite number and size we examined 5 female and 5 male 3xTg-AD mice aged 2 to 4, 13 to 15, and 18 to 20 month-old. ChAT-ir neurite number was determined by counting all immunopositive neurites within the cortex and hippocampus throughout an entire series of sections using a Nikon microscope at 60x magnification. Fiduciary landmarks were used to avoid counting the same object more than once. Quantification of age-related alterations in relative area (μm^2) of cortical and hippocampal ChAT dystrophic neurites was determined using female and male middle (13 months) and old (18-19 months) 3xTg-AD mouse using the Image 1.60 (Scion 1.6) program as previously described (Perez et al., 2007). One hundred ChAT-ir neurites from the cortex and hippocampus were randomly outlined and area measurements were automatically analyzed in gray-scale images. An observer blind to age, gender and genotype performed the quantitative analysis of ChAT-ir dystrophic neurite number and size.

ChAT radioenzymatic assay

Cortical and hippocampal tissue (n=75) harvested from the same young (2-3 months), middle age (13-15 months) and old (18-20 months) 3xTg-AD and age-matched ntg mice were processed for ChAT enzyme activity using a modification of the Fonnum method (DeKosky et al., 1992; Fonnum, 1975). Frozen tissue was homogenized using high frequency sonication in a solution containing 0.5% Triton X-100 and 10 mM EDTA. Briefly, 5 μl of tissue homogenate was combined with ^{14}C-labeled acetyl Co-A (New England Nuclear, Boston, MA), incubation buffer (100 mM sodium phosphate, 600 mM NaCl, 20 mM choline chloride, 10 mM disodium EDTA, pH7.4), and physostigmine (20 mM, Sigma, St. Louis, MO). After 30 minutes of incubation at 37°C in a water bath, the reaction was stopped by the addition of 4 ml of 10 mM phosphate buffer (pH 7.4). Subsequently, 1.6 ml of acetonitrile/tetraphenylboron mixture and 8 ml of scintillation fluid were added to cause phase separation, and the samples were allowed to stabilize for 24 hours before scintillation counting. Protein content of the samples was determined using a BCA protein assay kit (Pierce, Rockford, IL). ChAT enzyme activity was expressed as μmol/hr/g protein. Samples were coded, and all assays were performed in triplicate by a technician blinded to experimental groups.

Western immunoblotting

Antibodies—Rabbit polyclonal antibodies against proNGF (H-20, 1:50, Santa Cruz, CA, USA), p75^{NTR} (1:300, Abcam, Cambridge, MA) and TrkA (1:50; Fitzgerald Industries International, Inc, MA) were used for quantitative immunoblotting. A monoclonal antibody against β-actin (1:30,000, Sigma, St. Louis, MO) was used as an internal control for protein loading.

In the present study cases were mixed across genotype at each age for all western blot experiments. Tissue samples from cortex and hippocampus were processed for western blotting as previously reported (Counts et al., 2004). Tissues were sonicated in ice-cold homogenization buffer (20 mM Tris, 1mM EGTA, 1mM EDTA, 10% sucrose, pH 7.4) containing protease inhibitors (2 mg/ml leupeptin, 0.01 U/ml aprotinin, 1 mg/ml pepstatin A, 1 mg/ml antipain, 2.5 mg/ml chymostatin, 10 mM benzamidine, 0.1 mM phenylmethyl sulfonyl fluoride, 0.4 mg/ml N-p-Tosyl-L-phenylalanine chloromethyl ketone (TPCK), 0.4 mg/ml N-α-p-Tosyl-L-lysine chloromethyl ketone (TLCK), 0.4 mg/ml soybean trypsin inhibitor, 0.1 mM sodium fluoride, and 0.1 mM sodium orthovanadate). Supernatant S1 fractions were prepared by centrifugation at 1,000 rpm for 10 minutes at 4°C, and protein concentration was determined by the Bradford method (Bio-Rad, Hercules, CA). Sample proteins were denatured in sodium dodecyl sulfate (SDS) loading buffer to a final concentration of 5 mg/ml for TrkA and p75^{NTR} and 7.5 mg/ml for proNGF. Sample proteins (50 μg/sample for NGF receptors or 75 μg/sample for proNGF) were separated by SDS-polyacrylamide gel electrophoresis (PAGE; 7.5% acrylamide for TrkA and p75^{NTR}; gradient 8-16% acrylamide for proNGF) and transferred electrophoretically to polyvinylidene fluoride membranes (Immobilon P; Millipore, Billerica, MA). Membranes were blocked in TBS/0.1% Tween-20/5% milk for 30 minutes at room temperature. Subsequently, the top half of the membrane was incubated with rabbit TrkA antiserum (140 kDa), and the bottom half of the membrane was incubated simultaneously with rabbit anti-p75^{NTR} (75 kDa) and mouse anti-β-actin (42 kDa) antibodies in blocking buffer for 30-60 minutes at room temperature and then overnight at 4°C. A different membrane was used to probe the transferred samples with anti-proNGF and anti-β-actin antibodies in blocking buffer as described above. The following day, after several room-temperature rinses in TBS, blots were incubated for 1 hour at room temperature with either horseradish peroxidase (HRP)-conjugated goat anti-rabbit IgG secondary antibody (1:5000; Bio-Rad, PA) for detection of TrkA and p75^{NTR}, or HRP-conjugated goat anti-mouse IgG secondary antibody (1:8,000;

Pierce, Rockford, IL) for detection of proNGF and β-actin. Immunoreactive proteins were visualized by enhanced chemiluminescence (Amersham Biosciences, Piscataway, NJ) on a Kodak Image Station 440CF (Eastman Kodak, New Haven, Cincinnati, Ohio). Bands were quantified using Kodak 1D image analysis software (Perkin-Elmer, Wellesley, MA). No immunoreactive bands were detected on blots probed with the anti-rabbit or anti-mouse secondary IgG alone (data not shown). ProNGF, TrkA and $p75^{NTR}$-ir signals were normalized to β-actin signal for quantitative analysis. Each sample was analyzed three times in independent experiments, and the means were used for further analysis.

Statistical Analysis

Data from unbiased stereological counts, western blot and ChAT enzymatic assay that followed a Gaussian curve were statistically evaluated using *t*-test or three- and two-way analysis of variance (ANOVA), where interactions of genotype, age and/or gender were evaluated. Non-parametric data were examined with Mann-Whitney rank sum test or Kruskal-Wallis ANOVA rank test. Holm-Sidak and Dunn's post hoc test were used for multiple comparisons as appropriate. Correlation between coefficients was analyzed with a Spearman test. Data were represented as mean ± standard error of the mean (SEM). The level of statistical significance was set at 0.05, two-tailed. Data was analyzed using SigmaPlot 10.0 (Aspire Software International, Leesburg, VA).

RESULTS

Hippocampal and cortical cholinergic fiber dystrophy increases with age in 3xTg-AD mice

To examine the impact of Aβ plaque deposition upon cholinergic fibers in cortex and hippocampus, brain sections were single or double immunolabeled using the 6E10 and ChAT antibodies as described above. A description of the progression of cortical and hippocampal 6E10 immunoreactivity in 3xTg-AD mice derived from our colony has recently been reported (Oh et al., 2010). In brief, intraneuronal 6E10 staining and tau conformation isoforms were immunodetected as early as 3 weeks of age in the layer III and V of the cortex and CA1 hippocampal complex in both male and female 3xTg-AD mice (Oh et al., 2010). The cholinergic interneurons in the cortex and hippocampus were not immunoreactive for 6E10 or tau (data not shown). Cortical and hippocampal extraneuronal 6E10 positive plaques increased with age, and their expression is gender-dependent in 3xTg-AD mice (Fig. 1A-H). Specifically, female mutant mice show earlier and more accelerated plaque deposition than males, displaying Aβ deposits in the subiculum at 8-9 months (Fig. 1A-B) compared to 11-12 months of age for males (Oh et al., 2010). In addition, sections dual stained for 6E10 and thioflavine-S revealed that the majority of the plaques displayed both markers within the core of the plaque, while only 6E10-ir was seen at the periphery of the plaque (Fig. 1I-K).

Cortex and hippocampus displayed similar patterns of ChAT-ir fibers in both the 3xTg-AD and age-matched ntg mice (Fig. 2A-L). In the cortex, a fine network of ChAT-ir fibers was seen throughout all cortical layers (Fig. 2A, B). In the hippocampus, ChAT-ir fibers displayed the classic laminar distribution with a dense band in the hippocampal molecular layer as well as in the subiculum (Fig. 2E-L). In addition, there was no apparent difference in ChAT-ir fiber density in the cortex and hippocampus between young 3xTg-AD and ntg mice (Fig. 2A-D, E-L). However, we observed a qualitative decrease in the density of ChAT immunoreactivity in the subiculum of 18 to 20 months old female 3xTg-AD compared to age-matched ntg mice (see Fig. 3H and I), which was less obvious in the hippocampus proper. There was no an apparent reduction in cortical ChAT-ir fibers in 3xTg-AD mice in either gender (data not shown), although this will require a more systematic quantitative evaluation.

Examination of ChAT-ir fibers in the vicinity of cortical and hippocampal 6E10 and Alz50-ir neurons did not reveal alterations in their geometry or trajectory between young (Fig. 2A-M, O) and old (Fig. 2N and P) 3xTg-AD. ChAT-ir neurite formation was first observed within the subiculum in 8-10 months old female 3xTg-AD in association with Aβ deposits (data not shown). A similar pattern was not seen until 11-12 months of age in the subiculum of male 3xTg-AD mice. Hippocampal dystrophic ChAT-ir neurites were more conspicuous by 13 months in both male and female mutant mice compared to lack of dystrophic fibers in ntg mice (Fig. 3A-C). In general, cholinergic dystrophic swellings appeared in a rosette or grape-like pattern (Fig. 3D-G). A semi-quantitative evaluation revealed a significant age-related increase in hippocampal and cortical ChAT-ir dystrophic neurite number in female but not male mutant mice (Fig. 3J and K, Holm-Sidak post hoc and *t*-test, $p^*<0.05$). In addition, there was a 42% and 33% increase in hippocampal cholinergic dystrophic neurite area in 18-19 month- compared to 13 month-old female and male 3xTg-AD mice, respectively. Furthermore, there was a 34% increase in cortical ChAT-ir dystrophic neurite area in 18-19 month compared to 13 month-old female mutant mice. Sufficient numbers of cortical cholinergic neurites were found in male mutants to perform a quantitative analysis.

Loss of ChAT immunoreactive neurons in the medial septum/vertical limb of diagonal band of Broca in aged 3xTg-AD mice

The CBF complex is composed of the medial septum, vertical and horizontal limbs of the diagonal band of Broca and nucleus basalis of Meynert, which are the main sources of cholinergic innervation to the hippocampus and cortex, respectively (Amaral and Kurz, 1985; Mesulam et al., 1983). Since the hippocampal formation displays an earlier Aβ plaque deposition and cholinergic dystrophy than the cortex in 3xTg-AD tg mice (Oh et al., 2010), we examined cholinergic neurons number in the MS/VDB using an unbiased stereologic counting method (Fig. 4A-C). Interestingly, ChAT-ir neurons were not immunreactive for 6E10 (data not shown) or Alz50 and AT8 in the MS/VDB of 3xTg-AD mice (Fig. 4D and E). However, plaques (Fig. 4F and G) and Alz50 and AT8 positive dystrophic neurites (Fig. 4H-K) were present in the lateral septum in aged 3xTg-AD mice. A three-way ANOVA showed an age effect on the number of the ChAT-ir neurons in the MS/VDB ($p=0.011$). Post hoc analysis revealed a significant (23%) reduction in the number of ChAT-ir neurons in the MS/VDB between young and old 3xTg-AD mice (Fig. 4L, Holm-Sidak post hoc, $p^*<0.05$).

Cortical and hippocampal ChAT enzyme activity decrease in middle-aged 3xTg-AD mice

To examine changes with age in cholinergic metabolic activity, ChAT enzyme levels were evaluated in the cortex and hippocampus of young (2-3 months), middle-aged (13-15 months) and old (18-20 month) 3xTg-AD and age-matched ntg mice. Statistical analysis revealed a significant interaction between genotype and age with cortical ChAT activity (three-way ANOVA; $p=0.014$). Specifically, there was a significant increase in cortical ChAT activity in aged 3xTg-AD compared to middle age and young 3xTg-AD (Fig. 5A, Holm-Sidak $*p<0.05$). In aged ntg mice ChAT enzyme activity was significantly increased compared to young ntg mice (Fig. 5A, $*p<0.05$). In addition, cortical ChAT activity was significantly reduced in middle-aged 3xTg-AD mice compared to age-matched ntg mice, whereas no change was found between groups at the other time points examined (Fig. 5A, $*p<0.05$). Holm-Sidak multiple comparison test also revealed a significant reduction in hippocampal ChAT activity in middle-aged compared to young 3xTg-AD and middle-aged ntg mice (Fig. 5B, $*p<0.05$). No age-related changes in hippocampal ChAT activity were found in ntg mice (Fig. 5B, $p>0.05$).

Cortical proNGF levels increase in aged 3xTg-AD mice

To examine whether there are changes in the levels of cortical and hippocampal proNGF with age we examined young (2-3 months), middle-aged (13-15 months) and old (18-20

months) 3xTg-AD and age-matched ntg mice using quantitative western blot analysis. Cortical and hippocampal NGF levels were virtually undetectable using routine immunoblotting procedures in any mice examined at each age (data not shown). By contrast, cortical levels of proNGF, the precursor for NGF, were significantly increased in older compared to middle-aged and young 3xTg-AD mice (Fig. 6A and B, Kruskal-Wallis ANOVA on ranks, *$p<0.001$), whereas the levels of cortical proNGF in ntg mice were unchanged with age. In addition, hippocampal proNGF levels in both older 3xTg-AD and ntg mice were significantly increased compared to their respective middle-aged and young 3xTg-AD and ntg mice (Fig. 6C, Kruskal-Wallis ANOVA on ranks, *$p<0.001$), without significant changes between genotypes (Fig. 6C, Kruskal-Wallis ANOVA on ranks, $p>0.05$).

Gender differences in cortical and hippocampal TrkA levels in 3xTg-AD mice

To evaluate changes in cortical and hippocampal high- (TrkA) and low- ($p75^{NTR}$) affinity NGF receptor protein levels, we examined tissue from young (2-3 months), middle-aged (13-15 months) and old (18-20 months) 3xTg-AD and age matched ntg mice by quantitative western blotting. We found significant differences in cortical TrkA, but not $p75^{NTR}$ levels, between gender in young (Mann-Whitney rank sum test, $p=0.002$) and middle-aged (Mann-Whitney rank sum test, $p=0.002$) 3xTg-AD, as well as in young ntg mice (Mann-Whitney rank sum test, $p=0.004$). Since cortical TrkA levels in both genotypes displayed gender differences, data from male and female animals were analyzed separately. Statistical analysis revealed no changes in cortical TrkA levels with age in female 3xTg-AD mice (Fig. 7A, E, Kruskal-Wallis ANOVA on ranks, $p>0.05$). However, cortical TrkA levels in middle-aged female ntg mice were significantly increased compared to young female ntg mice (Fig. 7C, E, Kruskal-Wallis ANOVA on ranks, *$p< 0.01$). By contrast, we found a significant reduction in cortical TrkA levels in aged male compared to young 3xTg-AD mice (Fig. 7B, F, Kruskal-Wallis ANOVA on ranks, *$p< 0.01$), whereas cortical TrkA levels in male ntg mice were unchanged with age (Fig. 7D, F). No significant age-related differences were found in cortical $p75^{NTR}$ levels in 3xTg-AD mice. Cortical $p75^{NTR}$ levels of aged ntg mice, however, were significantly increased compared to middle-aged and young ntg mice (Fig. 7G, Kruskal-Wallis ANOVA on ranks, #$p<0.05$).

Hippocampal TrkA, but not $p75^{NTR}$ levels, were significantly different between genders within the following groups: young (Mann-Whitney rank sum test, $p=0.019$) and old (Mann-Whitney rank sum test, $p=0.017$) 3xTg-AD, as well as in old ntg (Mann-Whitney rank sum test, $p=0.026$) mice. There was a significant reduction of hippocampal TrkA in aged female 3xTg-AD compared to middle-aged female mutant mice (Fig. 8A, E, Kruskal-Wallis ANOVA on ranks, $^{\#}p<0.05$), whereas hippocampal TrkA levels in female ntg mice were unchanged across ages (Fig. 7C, E). Interestingly, hippocampal TrkA levels in middle-aged male 3xTg-AD mice were higher than middle-aged male ntg mice (Fig. 8B, D, F, Kruskal-Wallis ANOVA on ranks, *$p<0.01$), but neither male 3xTg-AD nor ntg mice showed changes in hippocampal TrkA levels with age (Fig. 8B, D, F). By contrast, hippocampal $p75^{NTR}$ levels in older 3xTg-AD were significantly increased compared to middle-aged mutant mice (Fig. 9A, C, Kruskal-Wallis ANOVA on ranks, *$p<0.01$), but no changes in $p75^{NTR}$ levels were detected with age in ntg mice (Fig. 9B and C).

Spearman correlation revealed a significant positive relationship between the NGF receptors, TrkA and $p75^{NTR}$, in the hippocampus in old 3xTg-AD mice ($r=0.769$, $p=0.00123$).

DISCUSSION

Cholinergic alterations in 3xTg-AD mice

The present study demonstrated that hippocampal and cortical cholinergic neuritic dystrophy increases in an age-dependent manner, which parallels the progression of Aβ plaque pathology in our cohort of 3xTg-AD mice (Oh et al., 2010), similar to other mouse models of AD (German et al., 2003; Perez et al., 2007). Swollen cholinergic dystrophic neurites were first seen at 8-10 months of age in close apposition to Aβ plaques within the subiculum of female compared to 11-12 month old male 3xTg-AD mice, coincident with a an earlier onset of plaques in female mutant mice (Hirata-Fukae et al., 2008; Oh et al., 2010). Cholinergic dystrophic neurites were not seen in the cortex or hippocampus of 2-3 months old 3xTg-AD mice, only few cortical cholinergic swellings appeared in 18-20 month-old female 3xTg-AD mice, and virtually none appeared in male 3xTg-AD mice. The number and size of ChAT-ir neurites in the cortex and hippocampus displayed an age-related increase, which was more conspicuous in female than in male 3xTg-AD mice. The age related increase in ChAT-positive neurites seen in 3xTg-AD support previous studies in other APP over-expressing mice (Boncristiano et al., 2002; Brendza et al., 2003; D'Amore et al., 2003; German et al., 2003; Hu et al., 2003; Hernandez et al., 2001; Perez et al., 2007). Cholinergic dystrophic neurites are associated with thioflavine-S-positive compact plaques (data not shown) in our 3xTg-AD mice (present findings) rather than diffuse plaques (Boncristiano et al., 2002; Brendza et al., 2003; D'Amore et al., 2003; German et al., 2003; Hu et al., 2003; Hernandez et al., 2001; Perez et al., 2007). In addition, cholinergic dystrophic neurites are the first type of the neurotransmitter system to display abnormalities in APP over-expressing mice (Bell et al., 2003, 2005; Hu et al., 2003), suggesting that cholinergi fibers are more susceptible to Aβ-induced dystrophy. The fact that cholinergic basal forebrain (CBF) neurons and hippocampal or cortical neurites do not co-express tau isoforms suggest that tau pathology does not play a direct role in the degeneration of the CBF system in these mutant mice. Swollen dystrophic neurites have been interpreted as aberrant sprouting consequent to Aβ deposition in APP over-expressing mice and in AD (Brendza et al., 2005; Ikonomovic et al., 2007; Lombardo et al., 2003). Others suggest that dystrophic neurites are the result of a compromised vesicular transport system, mostly related to fast axonal transport deficits (Piginio et al., 2003; Suzuki et al., 2006). Like other APP over-expressing mice (Luth et al., 2003; Masliah et al., 1996; Phinney et al., 1999), ultrastructural analysis of dystrophic swellings in 3xTg-AD mice revealed vesicular organelles (Oh et al., 2010), which have been implicated in endocytic (Cataldo et al., 2000; Mathews et al., 2002) and/or autophagic (Yang et al., 2008) processes. Defective autophagia mechanism (e.g. lysosome maturation) could delay the degradation of proteins involved in cell death, such as caspase-3 (Nixon 2007; Yang et al., 2008).

Unlike other studies, which reported stability of CBF neuron number in APP over-expressing mice (Boncristiano et al., 2002; German et al., 2003; Hernandez et al., 2001; Jaffar et al., 2001), here we report for the first time a 23% reduction in the number of cholinergic neurons in the MS/VDB of aged compared to young 3xTg-AD mice, whereas the number of cholinergic neurons did not change with age in ntg mice. This age-related reduction in CBF neuron number is due to the greater number of MS/VDB cholinergic neurons found in younger mutant animals. The reason for the increased number of cholinergic neurons in the young mutant mice is not clear. It is possible that the co-expression of the three FAD transgenes in this animal alters the development milieu resulting in a higher number of cholinergic MS/VDB neurons. However as the animals age, the developmental effects are paired-back resulting in a return to near normal CBF cell numbers. We are currently investigating whether there are phenotypic developmental changes related to the expression of the NGF receptors trkA and $p75^{NTR}$ within MS/VDB neurons in our 3xTg-AD mice. There is evidence that Aβ over expression can affect other

brain chemical systems, as well. For example, we reported an increase of striatal 3,4-dihydroxyphenylacetic acid (DOPAC) levels in APPswe/PS1ΔE9 tg mice at 3-6 months of age compared to ntg mice also suggesting a developmental and/or compensatory up-regulation of this dopamine metabolite in this APP over expressing mouse model of AD (Perez et al., 2005). Taken together these findings suggest the need to carefully examine the affect of the over expression of AD transgenes upon the developing central nervous system.

Interestingly, intraneuronal APP/Aβ or tau isoforms were not found in MS/VDB cholinergic neurons (present study) but hippocampal CA1, subicular and cortical neurons do contain various tau epitopes in 3xTg-AD mice (Oddo et al., 2003a,b; Oh et al., 2010). A recent study demonstrated that damage of the fornix, the major fiber pathway carrying cholinergic fibers arising from neurons within the medial septum, reduces Aβ immunoreactivity in the cingulate cortex, suggesting that septal cholinergic axonal projections transport Aβ/APP in 3xTg-AD mice (Robertson et al., 2009). The reason we did not find evidence for Aβ/APP within the MS/VDB cholinergic neurons using the 6E10 antibody remain unknown. It is possible that there is a rapid turned over or transport of Aβ/APP by the MS/VDB neurons, which, in turn, is undetectable using the current immunocytochemical procedure. By contrast, fimbria fornix transection did not affect APP levels and Aβ deposition in the hippocampus of APP/PS1 mice (Liu, et al., 2002) suggesting the importance of comparing differences between transgenetic strains. A recent immunocytochemistry study reported intraneuronal oligomergic Aβ in cortical neurons and in the intraneuronal space in the subiculum where Aβ plaques are first detected in 3xTg-AD mice (Hirata-Fukae et al., 2008). Since Aβ/oligomer aggregates are thought to be neurotoxic, profoundly affecting neural network function (Hartley et al., 1999; Walsh and Selkoe, 2007), the impact of oligomers upon cholinotrophic function remains an important area of investigation. Studies are currently being performed to test this hypothesis. We also observed a qualitative reduction in the density of cholinergic fibers in the hippocampal-subicular complex in aged 3xTg-AD mice, suggesting that a retrograde signal plays a key role in MS/VDB cholinergic cell degeneration in these triple transgenic mice. Although we did not perform cholinergic fiber counts, previous studies have shown an age-dependent loss of hippocampal and cortical cholinergic fibers in APP over-expressing transgenic mice (Aucoin et al., 2005; Boncristiano et al., 2002; German et al., 2003) reminiscent of the cortical cholinotrophic fiber depletion seen in human AD (Geula and Mesulam, 1996; Ikonomovic et al., 2007; Mufson et al., 1989), which results from CBF cell loss (Gilmor et al., 1999; Mufson et al., 2000, 2002 and 2008; Whitehouse et al., 1998).

Although we observed hippocampal cholinergic fiber dystrophy and MS/VDB cholinergic cell loss in aged 3xTg-AD mice, ChAT enzyme activity was not significantly reduced at this time point. In contrast, there was a significant reduction in ChAT activity in the hippocampus but not a loss of MS/VDB cholinergic neurons of middle-aged mutants, perhaps indicative of a down regulation of ChAT activity, which may precede the onset of cholinergic neuronal degeneration. On the other hand, cortical ChAT activity was significantly increased in aged compared to middle-aged and young 3xTg-AD mice. The factor(s) underlying the mismatch between the hippocampal and cortical cholinergic systems remains a curiosity. However, this is similar to the mismatch reported between ChAT activity levels and cholinergic fiber density in the superio frontal cortex decribed in prodromal and early AD subjects (Ikonomovic et al., 2007). A possible mechanism underlying this mismatch is an up-regulation of ChAT enzyme activity as reported in other transgenic mouse models of AD (Hernandez et al., 2001) as well as in people with prodromal AD (DeKosky et al., 2002; Ikonomovic et al., 2007). In both of these conditions there is an increase in swollen cholinergic fibers suggesting accumulation of ChAT at the terminal endings (German et al., 2003), which may result in either an increase or stability in enzyme activity. It is of particular note that plaque deposition is greater in the hippocampal

complex than in the cortex in 3xTg-AD mice (Oh et al., 2010), suggesting that a more substantial amyloid plaque load is required to trigger alterations in the cholinergic system in 3xTg-AD mice.

ProNGF and NGF receptor protein levels in 3xTg-AD mice

In the present study, proNGF, the precursor of NGF (Fahnestock et al., 2001), was the principal form of NGF expressed in the brains of both ntg and 3xTg-AD mice. Western blot analysis revealed that cortical, but not hippocampal, proNGF levels were significantly increased with age in 3xTg-AD mice. Specifically, a two-fold increase in cortical proNGF was observed in the oldest compared to youngest 3xTg-AD mice. NGF is produced in interneurons in the cortex and hippocampus (Conner and Varon, 1992) where it binds to its cognate receptors and is retrogradely transported to CBF neurons (Sobreviela et al., 1997). Although in the presence of TrkA, proNGF exhibits neurotrophic features like NGF (Fahnestock et al., 2004), several studies indicate that proNGF can also activate neuronal apoptotic pathways (Lee et al., 2001; Masoudi et al., 2009; Nykjaer et al., 2004) leading to neuronal death. Although the mechanism(s) associated with alterations in proNGF levels in aged 3xTg-AD is unknown, a possibility is that APP/Aβ production plays a pivotal role in proNGF regulation. In this regard, Down syndrome mouse models, which contain an increase in gene dosage and expression of the amyloid precursor protein (APP), show an increase in hippocampal NGF levels associated with compromised CBF axonal transport and atrophy of these neurons (Cooper et al., 2001; Salehi et al., 2006). Alternatively accumulation of proNGF may be initiated by Aβ induced dysfunction of the complex protease cascade responsible for NGF maturation and degradation in the extracellular space (Bruno et al., 2009; Bruno and Cuello, 2006; Cuello and Bruno, 2007). However, despite an increase in APP gene dosage and a greater Aβ plaque load in the hippocampal complex compared to the cortex in our triple transgenic mice, only cortical proNGF levels were increased in aged 3xTg-AD mice with respect to younger mutants, suggesting that Aβ plaque deposition is not a determining factor in regulating proNGF accumulation in 3xTg-AD mice. Alternatively, there may be a differential response of the hippocampus, compared to the cortex, to Aβ plaque load. Moreover, the reduction of MS/VDB CBF neurons, which project to the hippocampus (Mesulam et al., 1983) seen in aged 3xTg-AD mice, may be related to a defect in the retrograde transport of proNGF.

NGF receptor protein level in 3xTg-AD mice

Cortical and hippocampal NGF receptor levels of TrkA, but not $p75^{NTR}$, displayed gender differences in both 3xTg-AD and ntg mice. Specifically, cortical TrkA levels in young and middle-aged male 3xTg-AD were significantly higher than in age-matched female 3xTg-AD mice. Likewise, hippocampal TrkA levels in young and old male 3xTg-AD mice were higher than in their respective age-matched female counter parts. Although the mechanism underlying the gender differences in TrkA cortical and hippocampal complex protein levels are unknown, there are several possibilities. For example, there are gender-based temporal differences in the development of cortical and hippocampal Aβ plaques, but not tau, in 3xTg-AD (Oh et al., 2010; Hirata-Fukae et al., 2008). These differences appear to be related to differences in the status of select sex hormones such that androgen in males (Rosario et al., 2006) and estrogen and progesterone in females act either independently or interactively to regulate AD-like neuropathology in 3xTg-AD (Carroll et al., 2007). These observations suggest that these mutant mice may be useful as a tool to investigate the influence of hormonal status on the cholinotrophic system.

Similar to human AD (Counts et al., 2004), we found that cortical and hippocampal TrkA levels were down-regulated but $p75^{NTR}$ remained stable in aged male and female 3xTg-AD mice compared to gender matched younger mutant mice. The reduction in TrkA is

consistent with an accumulation of cortical proNGF in old mutant mice, indicating a disruption of this positive signaling pathway. Similarly, mouse models of Down's syndrome that mimic the cholinotrophic neuropathology of AD, accumulate NGF protein due to defective CBF neuron retrograde transport and show a reduction in the number of medial septal TrkA positive cells (Salehi et al., 2006). Thus, cortical accumulation of proNGF and a reduction in TrkA may reflect defective axonal transport in aged 3xTg-AD mice. The reduction in hippocampal TrkA levels seen in aged female 3xTg-AD mice could result in the reduction in MS/VDB CBF neurons in aged 3xTg-AD mice. Unlike the reduction of TrkA, hippocampal $p75^{NTR}$ levels were increased in aged 3xTg-AD mice compared to middle-aged transgenic mice, but were unchanged in the cortex of 3xTg-AD mice. In this regard, $p75^{NTR}$ binds proNGF with high affinity eliciting a proapoptotic signal (Lee et al., 2001; Nykjaer et al., 2004). Therefore, the increase in hippocampal $p75^{NTR}$ may represent a switch favoring apoptosis over survival pathways in the cholinotrophic septohippocampal system perhaps in response to a modest accumulation of proNGF. Furthermore, increased $p75^{NTR}$ coupled with exacerbated hippocampal Aβ pathology in triple transgenic mice (Costantini et al., 2005) is consistent with the suggestion that $p75^{NTR}$ facilitates Aβ-induced neurodegeneration (Knowles et al., 2009). These findings indicate that age-related changes in TrkA and/or $p75^{NTR}$ levels, which are also region- and gender-dependent and possibly related to Aβ pathology, may either independently or interactively regulate cholinotropic dysfunction in 3xTg-AD mice. Although tau pathology was not found in the CBF neurons in these mice, it remains to be determined whether other forms of tau dysregulation are responsible for retrograde transport defects and aberrant regulation of NGF receptors in these mutant mice.

Whether hippocampal and cortical cholinotrophic deficits affect cognitive function in 3xTg-AD remains to be determined. However, clinical pathological investigations indicate a shift within the cholinotrophic system from cell survival to cell death mechanisms during the progression of cognitive decline leading to AD (Mufson et al., 2008). Interestingly, a recent study demonstrated that treatment with an agonist of the muscarinic receptor M1 improved cognitive function and decreased hippocampal plaque pathology in 3xTg-AD supporting our observations of cholinotrophic dysfunction in these mice (Caccamo et al., 2006). More importantly a NGF gene therapy clinical trial reported provocative findings indicating that delivery of NGF directly into the cholinergic basal forebrain can induce CBF plasticity, cortical activation and improve/stabilize cognitive function in patients with mild AD (Tuszynski et al., 2005). Together these finding support the need for further investigation of the NGF cholinotrophic system in the 3xTg-AD mouse model.

CONCLUSIONS

We found age and gender dependent changes in the cholinotrophic system in 3xTg-AD mice. While stereology revealed a reduction in ChAT-positive cells in MS/VDB in old 3xTg-AD mice, ChAT enzyme activity only decreased significantly in the hippocampus in middle-aged 3xTg-AD mice. Western blots demonstrated an increase in cortical levels of proNGF and a reduction in cortical and hippocampal TrkA levels, which was gender-dependent in aged mutant mice, whereas $p75^{NTR}$ levels increased in hippocampus but remained unchanged in the cortex of aged 3xTg-AD mice. Although cholinotrophic changes in these mice did not fully replicate those seen in AD, they may provide a useful tool to investigate cholinotrophic dysfunction in the face of amyloid and perhaps tau pathology.

Acknowledgments

This work was supported by the Shapiro foundation and AG10688. The authors thank K. Schafernak for editing the manuscript.

References

Amaral DG, Kurz J. An analysis of the origins of the cholinergic and noncholinergic septal projections to the hippocampal formation of the rat. J Comp Neurol 1985;240:37–59. [PubMed: 4056104]

Arnold SE, Hyman BT, Flory J, Damasio AR, Van Hoesen GW. The topographical and neuroanatomical distribution of neurofibrillary tangles and neuritic plaques in the cerebral cortex of patients with Alzheimer's disease. Cereb Cortex 1991;1:103–16. [PubMed: 1822725]

Aucoin JS, Jiang P, Aznavour N, Tong XK, Buttini M, Descarries L, Hamel E. Selective cholinergic denervation, independent from oxidative stress, in a mouse model of Alzheimer's disease. Neuroscience 2005;132:73–86. [PubMed: 15780468]

Barrett GL, Bartlett PF. The p75 nerve growth factor receptor mediates survival or death depending on the stage of sensory neuron development. Proc Natl Acad Sci USA 1994;91:6501–5. [PubMed: 8022812]

Bell KF, de Kort GJ, Steggerda S, Shigemoto R, Ribeiro-da-Silva A, Cuello AC. Structural involvement of the glutamatergic presynaptic boutons in a transgenic mouse model expressing early onset amyloid pathology. Neurosci Lett 2003;353:143–7. [PubMed: 14664921]

Bell KF, Ducatenzeiler A, Ribeiro-da-Silva A, Duff K, Bennett DA, Cuello AC. The amyloid pathology progresses in a neurotransmitter-specific manner. Neurobiol Aging 2005;27:1644–57. [PubMed: 16271419]

Boncristiano S, Calhoun ME, Kelly PH, Pfeifer M, Bondolfi L, Stalder M, Phinney AL, Abramowski D, Sturchler-Pierrat C, Enz A, Sommer B, Staufenbiel M, Jucker M. Cholinergic changes in the APP23 transgenic mouse model of cerebral amyloidosis. J Neurosci 2002;22:3234–43. [PubMed: 11943824]

Brendza RP, Bacskai BJ, Cirrito JR, Simmons KA, Skoch JM, Klunk WE, Mathis CA, Bales KR, Paul SM, Hyman BT, Holtzman DM. Anti-Abeta antibody treatment promotes the rapid recovery of amyloid-associated neuritic dystrophy in PDAPP transgenic mice. J Clin Invest 2005;115:428–33. [PubMed: 15668737]

Brendza RP, O'Brien C, Simmons K, McKeel DW, Bales KR, Paul SM, Olney JW, Sanes JR, Holtzman DM. PDAPP; YFP double transgenic mice: a tool to study amyloid-beta associated changes in axonal, dendritic, and synaptic structures. J Comp Neurol 2003;456:375–83. [PubMed: 12532409]

Bruno MA, Cuello AC. Activity-dependent release of precursor nerve growth factor, conversion to mature nerve growth factor, and its degradation by a protease cascade. Proc Natl Acad Sci USA 2006;103:6735–40. [PubMed: 16618925]

Bruno MA, Leon WC, Fragoso G, Mushynski WE, Almazan G, Cuello AC. Amyloid beta-induced nerve growth factor dysmetabolism in Alzheimer disease. J Neuropathol Exp Neurol 2009;68:857–69. [PubMed: 19606067]

Bulbarelli A, Lonati E, Cazzaniga E, Re F, Sesana S, Barisani D, Sancini G, Mutoh T, Masserini M. TrkA pathway activation induced by amyloid-beta (Abeta). Mol Cell Neurosci 2009;40:365–73. [PubMed: 19162192]

Buttini M, Yu GQ, Shockley K, Huang Y, Jones B, Masliah E, Mallory M, Yeo T, Longo FM, Mucke L. Modulation of Alzheimer-like synaptic and cholinergic deficits in transgenic mice by human apolipoprotein E depends on isoform, aging, and overexpression of amyloid beta peptides but not on plaque formation. J Neurosci 2002;22:10539–48. [PubMed: 12486146]

Caccamo A, Oddo S, Billings LM, Green KN, Martinez-Coria H, Fisher A, LaFerla FM. M1 receptors play a central role in modulating AD-like pathology in transgenic mice. Neuron 2006;49:671–82. [PubMed: 16504943]

Carroll JC, Rosario ER, Chang L, Stanczyk FZ, Oddo S, LaFerla FM, Pike CJ. Progesterone and estrogen regulate Alzheimer-like neuropathology in female 3xTg-AD mice. J Neurosci 2007;27:13357–65. [PubMed: 18045930]

Cataldo AM, Peterhoff CM, Troncoso JC, Gomez-Isla T, Hyman BT, Nixon RA. Endocytic pathway abnormalities precede amyloid beta deposition in sporadic Alzheimer's disease and Down syndrome: differential effects of APOE genotype and presenilin mutations. Am J Pathol 2000;157:277–86. [PubMed: 10880397]

Chen L, Yamada K, Nabeshima T, Sokabe M. Alpha7 Nicotinic acetylcholine receptor as a target to rescue deficit in hippocampal LTP induction in beta-amyloid infused rats. Neuropharmacology 2006;50:254–68. [PubMed: 16324726]

Conner JM, Varon S. Distribution of nerve growth factor-like immunoreactive neurons in the adult rat brain following colchicine treatment. J Comp Neurol 1992;326:347–62. [PubMed: 1469118]

Cooper JD, Lindholm D, Sofroniew MV. Reduced transport of [125I] nerve growth factor by cholinergic neurons and down-regulated TrkA expression in the medial septum of aged rats. Neuroscience 1994;62:625–9. [PubMed: 7532836]

Cooper JD, Salehi A, Delcroix JD, Howe CL, Belichenko PV, Chua-Couzens J, Kilbridge JF, Carlson EJ, Epstein CJ, Mobley WC. Failed retrograde transport of NGF in a mouse model of Down's syndrome: reversal of cholinergic neurodegenerative phenotypes following NGF infusion. Proc Natl Acad Sci USA 2001;98:10439–44. [PubMed: 11504920]

Costantini C, Weindruch R, Della Valle G, Puglielli L. A TrkA-to-p75NTR molecular switch activates amyloid beta-peptide generation during aging. Biochem J 2005;391:59–67. [PubMed: 15966860]

Counts SE, Nadeem M, Wuu J, Ginsberg SD, Saragovi HU, Mufson EJ. Reduction of cortical TrkA but not p75(NTR) protein in early-stage Alzheimer's disease. Ann Neurol 2004;56:520–31. [PubMed: 15455399]

Coyle JT, Price DL, DeLong MR. Alzheimer's disease: a disorder of cortical cholinergic innervation. Science 1983;219:1184–90. [PubMed: 6338589]

Cuello AC, Bruno MA. The failure in NGF maturation and its increased degradation as the probable cause for the vulnerability of cholinergic neurons in Alzheimer's disease. Neurochem Res 2007;32:1041–5. [PubMed: 17404842]

D'Amore JD, Kajdasz ST, McLellan ME, Bacskai BJ, Stern EA, Hyman BT. In vivo multiphoton imaging of a transgenic mouse model of Alzheimer disease reveals marked thioflavine-S-associated alterations in neurite trajectories. J Neuropathol Exp Neurol 2003;62:137–45. [PubMed: 12578223]

Davies P. Neurotransmitter-related enzymes in senile dementia of the Alzheimer's type. Brain Res 1979;171:319–27. [PubMed: 37989]

Davies P, Maloney AJ. Selective loss of central cholinergic neurons in Alzheimer's disease. Lancet 1976;2:1403. [PubMed: 63862]

DeKosky ST, Harbaugh RE, Schmitt FA, Bakay RA, Chui HC, Knopman DS, Reeder TM, Shetter AG, Senter HJ, Markesbery WR. Cortical biopsy in Alzheimer's disease: diagnostic accuracy and neurochemical, neuropathological, and cognitive correlations. Intraventricular Bethanecol Study Group. Ann Neurol 1992;32:625–632.

DeKosky ST, Ikonomovic MD, Styren SD, Beckett L, Wisniewski S, Bennett DA, Cochran EJ, Kordower JH, Mufson EJ. Upregulation of choline acetyltransferase activity in hippocampus and frontal cortex of elderly subjects with mild cognitive impairment. Ann Neurol 2002;51:145–55. [PubMed: 11835370]

Fahnestock M, Michalski B, Xu B, Coughlin MD. The precursor pro-nerve growth factor is the predominant form of nerve growth factor in brain and is increased in Alzheimer's disease. Mol Cell Neurosci 2001;18:210–20. [PubMed: 11520181]

Fahnestock M, Yu G, Michalski B, Mathew S, Colquhoun A, Ross GM, Coughlin MD. The nerve growth factor precursor proNGF exhibits neurotrophic activity but is less active than mature nerve growth factor. J Neurochem 2004;89:581–92. [PubMed: 15086515]

Fombonne J, Rabizadeh S, Banwait S, Mehlen P, Bredesen DE. Selective vulnerability in Alzheimer's disease: amyloid precursor protein and p75(NTR) interaction. Ann Neurol 2009;65:294–303. [PubMed: 19334058]

Fonnum F. A rapid radiochemical method for the determination of choline acetyltransferase. J Neurochem 1975;24:407–09. [PubMed: 1113118]

Frade JM, Barde YA. Nerve growth factor: two receptors, multiple functions. Bioessays 1998;20:137–45. [PubMed: 9631659]

Garzon DJ, Fahnestock M. Oligomeric amyloid decreases basal levels of brain-derived neurotrophic factor (BDNF) mRNA via specific downregulation of BDNF transcripts IV and V in differentiated human neuroblastoma cells. J Neurosci 2007;27:2628–35. [PubMed: 17344400]

German DC, Yazdani U, Speciale SG, Pasbakhsh P, Games D, Liang CL. Cholinergic neuropathology in a mouse model of Alzheimer's disease. J Comp Neurol 2003;462:371–81. [PubMed: 12811807]

Geula C, Mesulam MM. Systematic regional variations in the loss of cortical cholinergic fibers in Alzheimer's disease. Cereb cortex 1996;6:165–77. [PubMed: 8670647]

Gilmor ML, Erickson JD, Varoqui H, Hersh LB, Bennett DA, Cochran EJ, Mufson EJ, Levey AI. Preservation of nucleus basalis neurons containing choline acetyltransferase and the vesicular acetylcholine transporter in the elderly with mild cognitive impairment and early Alzheimer's disease. J Comp Neurol 1999;411:693–704. [PubMed: 10421878]

Gundersen HJ, Bagger P, Bendtsen TF, Evans SM, Korbo L, Marcussen N, Moller A, Nielsen K, Nyengaard JR, Pakkenberg B, et al. The new stereological tools: disector, fractionator, nucleator and point sampled intercepts and their use in pathological research and diagnosis. APMIS 1988;96:857–81. [PubMed: 3056461]

Hartley DM, Walsh DM, Ye CP, Diehl T, Vasquez S, Vassilev PM, Teplow DB, Selkoe DJ. Protofibrillar intermediates of amyloid beta-protein induce acute electrophysiological changes and progressive neurotoxicity in cortical neurons. J Neurosci 1999;19:8876–84. [PubMed: 10516307]

Hernandez D, Sugaya K, Qu T, McGowan E, Duff K, McKinney M. Survival and plasticity of basal forebrain cholinergic systems in mice transgenic for presenilin-1 and amyloid precursor protein mutant genes. Neuroreport 2001;12:1377–84. [PubMed: 11388415]

Hirata-Fukae C, Li HF, Hoe HS, Gray AJ, Minami SS, Hamada K, Niikura T, Hua F, Tsukagoshi-Nagai H, Horikoshi-Sakuraba Y, Mughal M, Rebeck GW, LaFerla FM, Mattson MP, Iwata N, Saido TC, Klein WL, Duff KE, Aisen PS, Matsuoka Y. Females exhibit more extensive amyloid, but not tau, pathology in an Alzheimer transgenic model. Brain Res 2008;1216:92–103. 24. [PubMed: 18486110]

Holtzman DM, Li Y, Chen K, Gage FH, Epstein CJ, Mobley WC. Nerve growth factor reverses neuronal atrophy in a Down syndrome model of age-related neurodegeneration. Neurology 1993;43:2668–73. [PubMed: 8255474]

Hu L, Wong TP, Cote SL, Bell KF, Cuello AC. The impact of Abeta-plaques on cortical cholinergic and non-cholinergic presynaptic boutons in Alzheimer's disease-like transgenic mice. Neuroscience 2003;121:421–32. [PubMed: 14522000]

Huang EJ, Reichardt LF. Neurotrophins: roles in neuronal development and function. Annu Rev Neurosci 2001;24:677–736. [PubMed: 11520916]

Ikonomovic MD, Abrahamson EE, Isanski BA, Wuu J, Mufson EJ, DeKosky ST. Superior frontal cortex cholinergic axon density in mild cognitive Impairment and early Alzheimer's Disease. Arch Neurol 2007;64:1312–7. [PubMed: 17846271]

Jaffar S, Counts SE, Ma SY, Dadko E, Gordon MN, Morgan D, Mufson EJ. Neuropathology of mice carrying mutant APP (swe) and/or PS1 (M146L) transgenes: alterations in the p75(NTR) cholinergic basal forebrain septohippocampal pathway. Exp Neurol 2001;170:227–43. [PubMed: 11476589]

Knowles JK, Rajadas J, Nguyen TV, Yang T, LeMieux MC, Vander Griend L, Ishikawa C, Massa SM, Wyss-Coray T, Longo FM. The p75 neurotrophin receptor promotes amyloid-beta(1-42)-induced neuritic dystrophy in vitro and in vivo. J Neurosci 2009;29:10627–37. [PubMed: 19710315]

Lad SP, Neet KE, Mufson EJ. Nerve growth factor: structure, function and therapeutic implications for Alzheimer's disease. Curr Drug Targets CNS Neurol Disord 2003;2:315–34. [PubMed: 14529363]

Lee R, Kermani P, Teng KK, Hempstead BL. Regulation of cell survival by secreted proneurotrophins. Science 2001;294:1945–8. [PubMed: 11729324]

Liu L, Ikonen S, Tapiola T, Tanila H, van Groen T. Fimbria-fornix lesion does not affect APP levels and amyloid deposition in the hippocampus of APP+PS1 double transgenic mice. Exp Neurol 2002;177:565–74. [PubMed: 12429202]

Lombardo JA, Stern EA, McLellan ME, Kajdasz ST, Hickey GA, Bacskai BJ, Hyman BT. Amyloid-beta antibody treatment leads to rapid normalization of plaque-induced neuritic alterations. J Neurosci 2003;23:10879–883. [PubMed: 14645482]

Luth HJ, Apelt J, Ihunwo AO, Arendt T, Schliebs R. Degeneration of beta-amyloid-associated cholinergic structures in transgenic APP SW mice. Brain Res 2003;977:16–22. [PubMed: 12788508]

Masliah E, Sisk A, Mallory M, Mucke L, Schenk D, Games D. Comparison of neurodegenerative pathology in transgenic mice overexpressing V717F beta-amyloid precursor protein and Alzheimer's disease. J Neurosci 1996;16:5795–811. [PubMed: 8795633]

Masoudi R, Ioannou MS, Coughlin MD, Pagadala P, Neet KE, Clewes O, Allen SJ, Dawbarn D, Fahnestock M. Biological activity of nerve growth factor precursor is dependent upon relative levels of its receptors. J Biol Chem 2009;284:18424–33. [PubMed: 19389705]

Mastrangelo MA, Bowers WJ. Detailed immunohistochemical characterization of temporal and spatial progression of Alzheimer's disease-related pathologies in male triple-transgenic mice. BMC Neurosci 2008;9:81. [PubMed: 18700006]

Mathews PM, Guerra CB, Jiang Y, Grbovic OM, Kao BH, Schmidt SD, Dinakar R, Mercken M, Hille-Rehfeld A, Rohrer J, Mehta P, Cataldo AM, Nixon RA. Alzheimer's disease-related overexpression of the cation-dependent mannose 6-phosphate receptor increases Abeta secretion: role for altered lysosomal hydrolase distribution in beta-amyloidogenesis. J Biol Chem 2002;277:5299–307. [PubMed: 11551970]

Mesulam MM, Mufson EJ, Levey AI, Wainer BH. Cholinergic innervation of cortex by the basal forebrain: cytochemistry and cortical connections of the septal area, diagonal band nuclei, nucleus basalis (substantia innominata), and hypothalamus in the rhesus monkey. J Comp Neurol 1983;214:170–97. [PubMed: 6841683]

Mufson EJ, Bothwell M, Kordower JH. Loss of nerve growth factor receptor-containing neurons in Alzheimer's disease: a quantitative analysis across subregions of the basal forebrain. Exp Neurol 1989;105:221–32. [PubMed: 2548888]

Mufson EJ, Counts SE, Perez SE, Ginsberg SD. Cholinergic system during the progression of Alzheimer's disease: therapeutic implications. Expert Rev Neurother 2008;8:1703–18. [PubMed: 18986241]

Mufson EJ, Ma SY, Cochran EJ, Bennett DA, Beckett LA, Jaffar S, Saragovi HU, Kordower JH. Loss of nucleus basalis neurons containing trkA immunoreactivity in individuals with mild cognitive impairment and early Alzheimer's disease. J Comp Neurol 2000;427:19–30. [PubMed: 11042589]

Mufson EJ, Ma SY, Dills J, Cochran EJ, Leurgans S, Wuu J, Bennett DA, Jaffar S, Gilmor ML, Levey AI, Kordower JH. Loss of basal forebrain P75(NTR) immunoreactivity in subjects with mild cognitive impairment and Alzheimer's disease. J Comp Neurol 2002;443:136–53. [PubMed: 11793352]

Nagele RG, D'Andrea MR, Anderson WJ, Wang HY. Intracellular accumulation of beta-amyloid (1-42) in neurons is facilitated by the alpha 7 nicotinic acetylcholine receptor in Alzheimer's disease. Neuroscience 2002;110:199–211. [PubMed: 11958863]

Nixon RA. Autophagy, amyloidogenesis and Alzheimer disease. Cell Sci 2007;120:4081–91.

Nykjaer A, Lee R, Teng KK, Jansen P, Madsen P, Nielsen MS, Jacobsen C, Kliemannel M, Schwarz E, Willnow TE, Hempstead BL, Petersen CM. Sortilin is essential for proNGF-induced neuronal cell death. Nature 2004;427:843–8. [PubMed: 14985763]

Oddo S, Billings L, Kesslak JP, Cribbs DH, LaFerla FM. Abeta immunotherapy leads to clearance of early, but not late, hyperphosphorylated tau aggregates via the proteasome. Neuron 2004;43:321–32. [PubMed: 15294141]

Oddo S, Caccamo A, Kitazawa M, Tseng BP, LaFerla FM. Amyloid deposition precedes tangle formation in a triple transgenic model of Alzheimer's disease. Neurobiol Aging 2003a;24:1063–70. [PubMed: 14643377]

Oddo S, Caccamo A, Shepherd JD, Murphy MP, Golde TE, Kayed R, Metherate R, Mattson MP, Akbari Y, LaFerla FM. Triple-transgenic model of Alzheimer's disease with plaques and tangles: intracellular Abeta and synaptic dysfunction. Neuron 2003b;39:409–21. [PubMed: 12895417]

Oh K-J, Perez SE, Lagalwar S, Vana L, Binder L, Mufson EJ. Staging of Alzheimer's pathology in triple transgenic mice: a light and electron microscopic analysis. Int J AD. 2010 epub.

Overk CR, Kelley CM, Mufson EJ. Brainstem Alzheimer's-like pathology in the triple transgenic mouse model of Alzheimer's disease. Neurobiol Dis 2009;35:415–25. [PubMed: 19524671]

Paxinos, G.; Franklin, KBJ. The mouse brain in stereotaxic coordinates. 2nd ed.. Academic Press; San Diego: 2001.

Perez SE, Dar S, Ikonomovic MD, DeKosky ST, Mufson EJ. Cholinergic forebrain degeneration in the APPswe/PS1DeltaE9 transgenic mouse. Neurobiol Dis 2007;28:3–15. [PubMed: 17662610]

Perez SE, Lazarov O, Koprich JB, Chen EY, Rodriguez-Menendez V, Lipton JW, Sisodia SS, Mufson EJ. Nigrostriatal dysfunction in familial Alzheimer's disease-linked APPswe/PS1DeltaE9 transgenic mice. J Neurosci 2005;25:10220–9. [PubMed: 16267229]

Perry EK, Tomlinson BE, Blessed G, Bergmann K, Gibson PH, Perry RH. Correlation of cholinergic abnormalities with senile plaques and mental test scores in senile dementia. Br Med J 1978;2:1457–59. [PubMed: 719462]

Phinney AL, Deller T, Stalder M, Calhoun ME, Frotscher M, Sommer B, Staufenbiel M, Jucker M. Cerebral amyloid induces aberrant axonal sprouting and ectopic terminal formation in amyloid precursor protein transgenic mice. J Neurosci 1999;19:8552–9. [PubMed: 10493755]

Pigino G, Morfini G, Pelsman A, Mattson MP, Brady ST, Busciglio J. Alzheimer's presenilin 1 mutations impair kinesin-based axonal transport. J Neurosci 2003;23:4499–4508. [PubMed: 12805290]

Richter JA, Perry EK, Tomlinson B. Acetylcholine and choline levels in post-mortem human brain tissue: preliminary observations in Alzheimer's disease. Life Sci 1980;26:1683–89. [PubMed: 7392805]

Robertson RT, Baratta J, Yu J, LaFerla FM. Amyloid-beta expression in retrosplenial cortex of triple transgenic mice: relationship to cholinergic axonal afferents from medial septum. Neuroscience 2009;164:1334–46. [PubMed: 19772895]

Rosario ER, Carroll JC, Oddo S, LaFerla FM, Pike CJ. Androgens regulate the development of neuropathology in a triple transgenic mouse model of Alzheimer's disease. J Neurosci 2006;26:13384–9. [PubMed: 17182789]

Salehi A, Delcroix JD, Belichenko PV, Zhan K, Wu C, Valletta JS, Takimoto-Kimura R, Kleschevnikov AM, Sambamurti K, Chung PP, Xia W, Villar A, Campbell WA, Kulnane LS, Nixon RA, Lamb BT, Epstein CJ, Stokin GB, Goldstein LS, Mobley WC. Increased App expression in a mouse model of Down's syndrome disrupts NGF transport and causes cholinergic neuron degeneration. Neuron 2006;51:29–42. [PubMed: 16815330]

Seo H, Isacson O. Abnormal APP, cholinergic and cognitive function in Ts65Dn Down's model mice. Exp Neurol 2005;193:469–80. [PubMed: 15869949]

Sobreviela T, Clary DO, Reichardt LF, Brandabur MM, Kordower JH, Mufson EJ. TrkAimmunoreactive profiles in the central nervous system: colocalization with neurons containing p75 nerve growth factor receptor, choline acetyltransferase, and serotonin. J Comp Neurol 1994;350:587–611. [PubMed: 7890832]

Suzuki T, Araki Y, Yamamoto T, Nakaya T. Trafficking of Alzheimer's disease-related membrane proteins and its participation in disease pathogenesis. J Biochem 2006;139:949–55. [PubMed: 16788045]

Tuszynski MH, Thal L, Pay M, Salmon DP, U HS, Bakay R, Patel P, Blesch A, Vahlsing HL, Ho G, Tong G, Potkin SG, Fallon J, Hansen L, Mufson EJ, Kordower JH, Gall C, Conner J. A phase 1 clinical trial of nerve growth factor gene therapy for Alzheimer disease. Nat Med 2005;11:551–5. [PubMed: 15852017]

Walsh DM, Selkoe DJ. A beta oligomers - a decade of discovery. J Neurochem 2007;101:1172–84. [PubMed: 17286590]

Wang HY, Lee DH, D'Andrea MR, Peterson PA, Shank RP, Reitz AB. Beta-Amyloid(1-42) binds to alpha7 nicotinic acetylcholine receptor with high affinity. Implications for Alzheimer's disease pathology. J Biol Chem 2002;275:5626–32. [PubMed: 10681545]

West MJ. New stereological methods for counting neurons. Neurobiol Aging 1993;14:275–85. [PubMed: 8367009]

Whitehouse PJ, Price DL, Clark AW, Coyle JT, DeLong MR. Alzheimer disease: evidence for selective loss of cholinergic neurons in the nucleus basalis. Ann Neurol 1981;10:122–26. [PubMed: 7283399]

Whitehouse PJ, Struble RG, Hedreen JC, Clark AW, Price DL. Alzheimer's disease and related dementias: selective involvement of specific neuronal systems. CRC Crit Rev Clin Neurobiol 1985;1:319–39. [PubMed: 2876845]

Wilcock GK, Esiri MM, Bowen DM, Smith CC. Alzheimer's disease. Correlation of cortical choline acetyltransferase activity with the severity of dementia and histological abnormalities. J Neurol Sci 1982;57:407–17. [PubMed: 7161627]

Wong TP, Debeir T, Duff K, Cuello AC. Reorganization of cholinergic terminals in the cerebral cortex and hippocampus in transgenic mice carrying mutated presenilin-1 and amyloid precursor protein transgenes. J Neurosci 1999;19:2706–16. [PubMed: 10087083]

Yaar M, Zhai S, Pilch PF, Doyle SM, Eisenhauer PB, Fine RE, Gilchrest BA. Binding of beta-amyloid to the p75 neurotrophin receptor induces apoptosis. A possible mechanism for Alzheimer's disease. J Clin Invest 1997;100:2333–40. [PubMed: 9410912]

Yang DS, Kumar A, Stavrides P, Peterson J, Peterhoff CM, Pawlik M, Levy E, Cataldo AM, Nixon RA. Neuronal apoptosis and autophagy cross talk in aging PS/APP mice, a model of Alzheimer's disease. Am J Pathol 2008;173:665–81. [PubMed: 18688038]

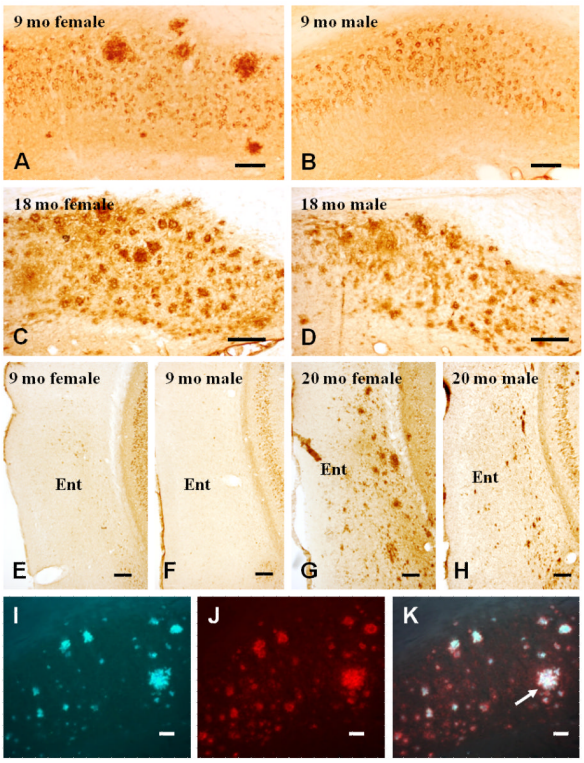

Figure 1.

A-H. Brightfield photographs showing the age and gender related progression of subicular and cortical 6E10 immunoreactive (ir) plaque deposition in 3xTg-AD mice. Panel **A** shows few 6E10-ir plaques and numerous immunopositive neurons in the subiculum of a 9 month-old female 3xTg-AD mouse compared to the subiculum (**B**) of an age-matched male 3xTg-AD mouse. **C-D**. Subiculum showing numerous 6E10-ir plaques in an 18 month-old female (C) compared to a male (**D**) 3xTg-AD mouse. **E-H**. Enthorhinal cortex lacks 6E10-ir deposits in both female (**E**) and male (**F**) 9 month-old 3xTg-AD mice compared to that seen in at 20 months of age in a female (**G**) and male (**H**) 3xTg-AD mouse. Note that the aged female (**G**) showing many more amyloid deposits than the aged male (**H**) mutant mouse. Single thioflavine-S (**I**) and 6E10 (**J)** staining in the subiculum of an 18 month-old female 3xTg-AD mouse. **K**. Merged image showing the co-localization of both markers in the plaque core (white; arrow) whereas the periphery was only 6E10 positive (red). Abbreviations: Ent, entorhinal cortex. Scale bars in A,B, I-K= 50 μm and C-H=100 μm.

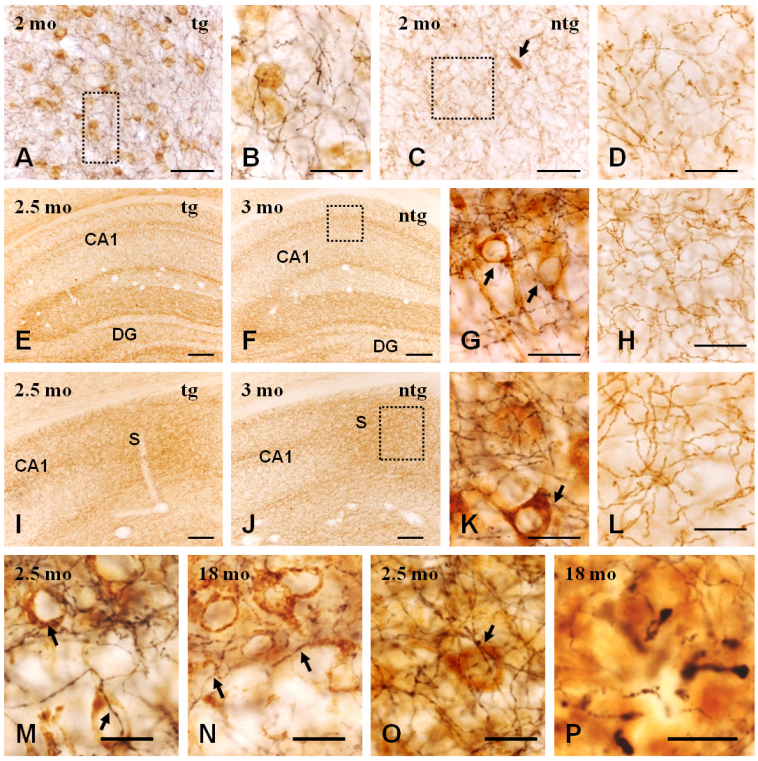

Figure 2.

Brightfield photographs showing ChAT-ir fibers and 6E10-ir neurons in the cingulate cortex and hippocampus in 2-3 month-old 3xTg-AD and age-matched ntg mice. **A**. Low magnification image of a section dual stain for ChAT-ir fibers (blue) and 6E10-ir neurons (brown) in the cingulate cortex of a 2 month-old 3xTg-AD mouse. **B**. Higher magnification image of the boxed area in panel **A** showing the normal appearance of the fine ChAT-ir fibers (blue) in the cingulate cortex. **C**. Low power image of tissue stained only for ChAT-ir profiles (brown) in the cingulate cortex of a 2 month-old ntg mouse. Note the presence of a ChAT-ir cortical interneuron (arrow). **D**. High power image of the boxed area in **C** showing similar morphology of cholinergic fibers in a 2 month-old age-matched ntg compared to the mutant mouse (see panels **A**, **B**). **E** and **F**. Low magnification of the dorsal hippocampal images showing no differences in the laminar organization of ChAT-ir fibers between young 3xTg-AD and ntg mice, respectively. **G**. ChAT-ir fibers (black) running in close apposition to 6E10-ir CA1 hippocampal pyramidal neurons (brown; arrows) showing no alterations in their trajectory or geometry in a young 3xTg-AD. **H**. High power image of area outlined in **F** showing similar ChAT-ir fiber organization in the CA1 field of the hippocampus in 3 month old 3xTg-AD and ntg mouse (**G**). **I** and **J**. ChAT-ir fibers within the CA1 field of the hippocampus and subiculum of young 3xTg-AD and ntg mice. Note the similarities of the cholinergic innervation pattern between genotypes. **K**. ChAT-ir fibers (black) in association with 6E10-ir neurons (brown, arrow) in the subiculum of a 3 month-old 3xTg-AD mouse. **L**. Higher-power image of boxed area in **J** showing similar ChAT-ir fiber organization to that seen in the subiculum of an age-matched 3xTg mouse. **M** and N. Hippocampal CA1 pyramidal neurons showing ChAT-ir fibers (black) in close apposition to Alz50-ir neurons (brown) in a young and old 3xTg-AD mouse. Note that alterations in trajectory or geometry of the cholinergic fibers (arrows) were not seen at either age. **O**. Subiculum showing no alterations in trajectory or geometry of the cholinergic fibers (black; arrow) in the proximity of an Alz50-ir neuron (brown) in a young 3xTg-AD mouse. **P**. Subicular ChAT-ir bulbous swellings (black) in the vicinities of a plaque in an 18 month-old 3xTg-AD mouse.

Abbreviations: CA1, field CA1 of the hippocampus; DG, dentate gyrus; ntg, non-transgenic mice; tg, 3xTg-AD transgenic mice; mo, months; S, subiculum. Scale bars in A,C= 30 μm, B, D, K, L, M-O= 15 μm, E, F, I, J = 100 μm, G, H= 20 μm and P=10 μm

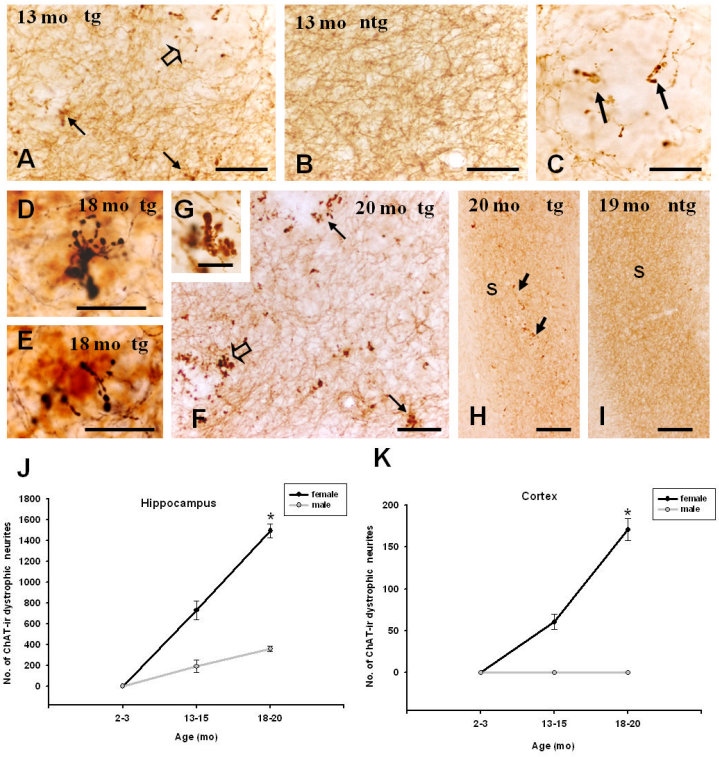

Figure 3.

Photographs showing ChAT-ir fibers and Aβ-ir plaques in the subiculum at 13 and 18-month old 3xTg-AD and aged ntg mice. **A**. Note the reduction in ChAT-ir fibers and neuritic swellings (black arrows) in the dorsal subiculum in a 13 month-old mutant compared to an age-matched ntg mouse (**B**). **C**. Photomicrograph of area adjacent to the open arrow in panel **A,** showing swollen dystrophic cholinergic neurites (arrows) adjacent to an imunonegative region indicative of Aβ plaque damage. **D** and **E**. Subicular Aβ-ir plaques innervated by grape-like clusters of bulbous swollen ChAT-ir dystrophic neurites in an 18 month-old mutant mouse. **F**. Dorsal subiculum displayed many more ChAT-ir fiber swellings (black arrows) at 20 months of age compared to a 13 month-old mutant mouse (see panel **A**). **G**. Detail of a cluster of ChAT-ir dystrophic neurites adjacent to the open arrow shown in **F**. **H** and **I**. Ventral subiculum displayed a marked reduction in ChAT staining and numerous ChAT-ir dystrophic neurites (black arrows) in a 20 month-old female mutant compared to a 19 month-old female ntg mouse, respectively. **J** and K. Linear graphs illustrating the mean values of the ChAT-ir dystrophic neurite number in the hippocampus and the cerebral cortex of 2 to 3, 13 to 15 and 18 to 20- month-old male and female 3xTg-AD mice. Statistical analysis revealed a significant increase in the number of cholinergic swellings in the hippocampus (**J**) and cortex (**K**) in aged female (18-20 months) compared to 13-15 months old 3xTg-AD mice, but no significant changes were found in the hippocampus (**J**) or cortex (**K**) in male 3xTg-AD mice. (*p values <0.05, hippocampal data was analyzed with a two-way ANOVA followed by Holm-Sidak post hoc and cortical data was analyzed with a *t*-student test). Abbreviations: ntg, non-transgenic mice; tg, 3xTg-AD transgenic mice; mo, months; S, subiculum. Scale bars in A,B = 30 μm, C,D,E = 20 μm, F,H,I= 100 μm and G =10 μm.

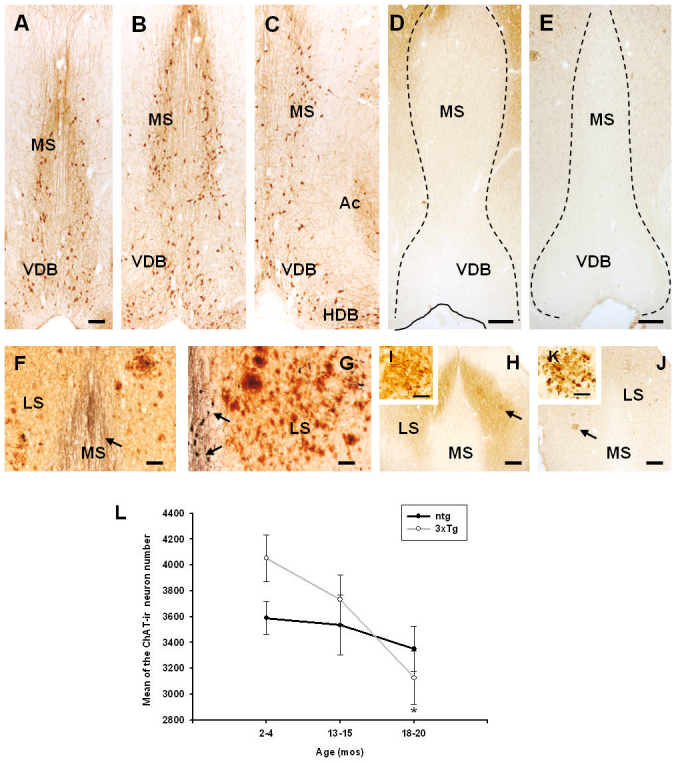

Figure 4.

A-C. Representative images showing the rostral to caudal levels of the forebrain containing the medial septum/vertical limb of the diagonal band of Broca (MS/VDB) ChAT-ir neurons analyzed using unbiased stereology from a 3 month-old ntg mouse. **D** and **E**. Low power images showing the absence of Alz50-ir (**D**) and AT8-ir (**E**) neurons within the MS/VDB in an 18 month-old female 3xTg-AD mouse. **F** and **G**. ChAT-ir fibers and cells (arrows, black) in the medial septum (MS) and Aβ-ir plaques (brown) in the lateral septum (LS) in 18 and 20-months old female 3Tg-AD mice, respectively. Note the increase in plaques in the 20 month-old mutant mouse. **H-K**. Images showing the lack of Alz50-ir and AT8-ir neurons in the lateral septum of a 18 month-old female mutant mouse and the presence of Alz50-ir dystrophic neurites and fibers (**H**) as well as AT8-ir dystrophic neurites (**J**) in intermediate aspects of the LS. **I** and **K**. High power photomicrographs of areas adjacent to the arrows showing swollen ALz50-ir and AT8-ir dystrophic neuritis, respectively. **L**. Linear representation of mean values of total ChAT-ir neuron numbers in the MS/VDB in 2-4, 13-15 and 18-20 month-old 3xTg-AD and age-matched ntg mice. Statistical analysis revealed a decrease in ChAT-ir neuron numbers in aged 3xTg-AD mice compared to young mutants, but unchanged in ntg mice across ages. (*p values <0.05, data was analyzed with a three-way ANOVA followed by Holm-Sidak post hoc test). Error bars=standard error of the mean. Abbreviations: 3xTg, 3xTg-AD transgenic mice; Ac, nucleus accumbens, ntg, non-transgenic mice; HDB, horizontal limb of the diagonal band of Broca; LS, lateral septum; MS, medial septum; mo, months; VDB, vertical limb of diagonal band of Broca. Scale bars in A-E, H, J=100μm, F and G=50 μm and I, J= 20 μm.

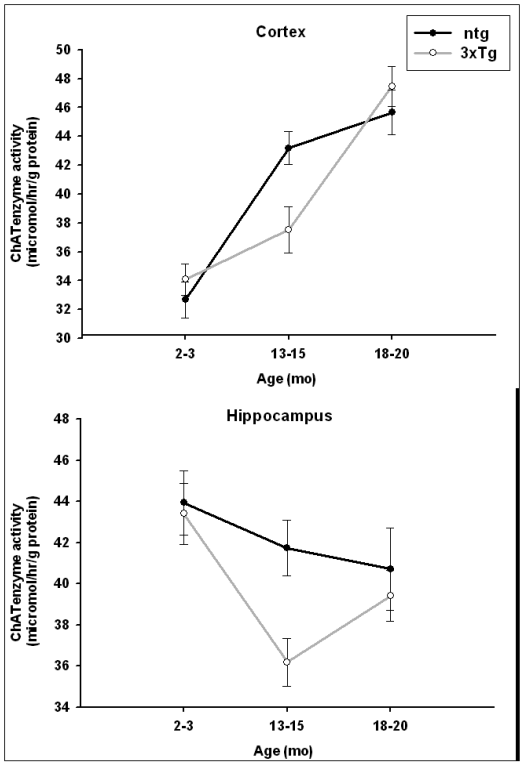

Figure 5.

Linear graphs illustrating the mean values of the ChAT enzyme activity (μmol/hr/g protein) in the cerebral cortex (**A**) and hippocampus (**B**) of 2 to 3, 13 to 15 and 18 to 20 month-old 3xTg-AD mice and ntg. **A**. Statistical analysis revealed a significant increase in cortical ChAT enzyme activity in 18-20 month-old 3xTg-AD compared to 2-3 and 13-15 month-old mutant mice. Statistical evaluation also revealed significant differences in cortical ChAT enzyme activity at 13-15 months between 3xTg-AD and ntg mice. Aged ntg mice showed a significant increased in ChAT activity compared to young ntg mice. **B**. Significant decrease in hippocampal ChAT activity was detected between 2-3 and 13-15 month-old 3xTg-AD mice, but no changes were found between ntg mice across ages. (*p values <0.05, data was analyzed with a three-way ANOVA followed by Holm-Sidak post hoc test for multiple comparisons). Abbreviations, ntg, non-transgenic mice; 3xTg, 3xTg-AD transgenic mice; error bars=standard error of the mean; mo, months.

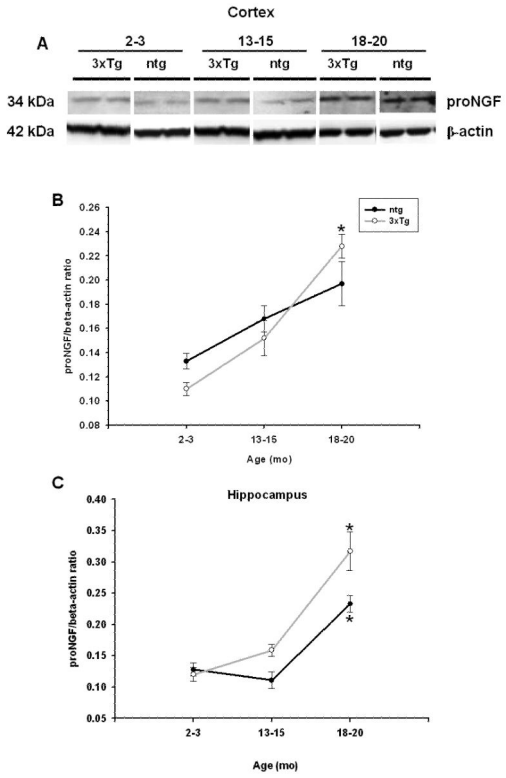

Figure 6.

A. Representative immunoblot from the cortex of 2 to 3, 13 to 15 and 18 to 20 month-old 3xTg-AD and ntg probed with antibodies against proNGF and β-actin. **B** and **C**. Linear representation of mean densitometry measurements of cortical (**C**) and (**B**) hippocampal proNGF-ir signals normalized to β-actin-ir in 2 to 3, 13 to 15 and 18 to 20 month-old 3xTg-AD and age-matched ntg mice. Statistical analysis revealed higher levels of proNGF in the cortex of aged 3xTg-AD mice compared to middle-aged and young mutant mice, but unchanged in ntg mice. In addition, hippocampal normalized proNGF-ir levels were significantly increased in both aged 3xTg-AD and ntg mice compared to their respective middle-aged and young 3xTg-AD and ntg mice (*p=<0.001, data was analyzed with a Kruskal-Wallis non-parametric test followed by Dunn's post hoc test for multiple comparisons). Abbreviations: ntg, non-transgenic mice; 3xTg, 3xTg-AD transgenic mice; error bars=standard error of the mean; mo, months.

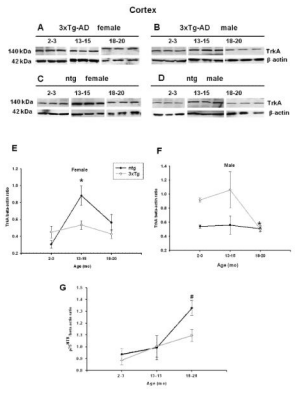

Figure 7.

A-D. Representative cortical immunoblots probed with antibodies against TrkA and β-actin in female and male 2 to 3, 13 to 15 and 18 to 20 month-old 3xTg-AD and ntg mice. **E** and **F**. Linear analysis of mean densitometry measurements showing no change in cortical TrkA-ir in female (**E**) and (**F**) male 3xTg-AD and ntg mice with signal normalized to β-actin-ir, whereas TrkA levels were significantly lower in aged male 3xTg-AD mice compared to the younger male mutants. Statistical analysis revealed that the levels of TrkA in middle-aged female ntg mice were increased significantly compared to young female ntg mice. **G**. Linear analysis of mean densitometry measurements for cortical $p75^{NTR}$-ir signals normalized to β-actin-ir in mutant and ntg mice revealed no changes with age in 3xTg-AD mice. There was a significant increased in $p75^{NTR}$ levels in aged ntg mice compared to middle-aged and young ntg mice. (*$p<0.01$ and #, $p<0.05$, data was analyzed with a Kruskal-Wallis non-parametric test follow by Dunn's post hoc test for multiple comparisons). Abbreviations: ntg, non-transgenic mice; 3xTg, 3xTg-AD transgenic mice; error bars=standard error of the mean; mo, months.

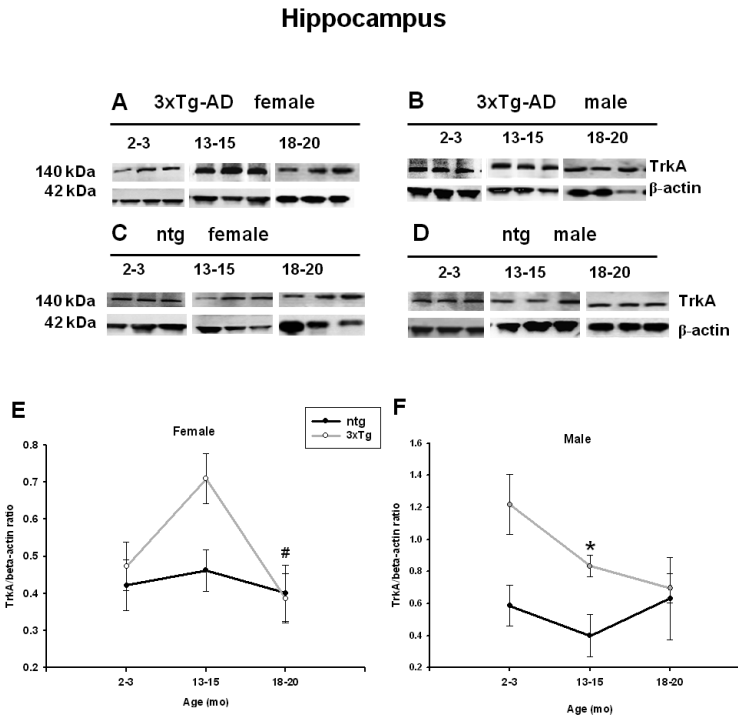

Figure 8.

A-D. Representative immunoblots from hippocampus of female and male 2 to 3, 13 to 15 and 18 to 20 month-old 3xTg-AD and ntg mice probed with antibodies against TrkA and β-actin. Note the decrease in TrkA immunoreactivity in aged female mutant mice (**A**) and stable hippocampal TrkA imunoreactivity in males (**B**) across age. **E** and **F.** Linear representation of mean densitometry measurements from hippocampal female (**E**) and male (**F**) TrkA-ir signals normalized to β-actin-immunoreactivity in 3xTg-AD and ntg mice. Statistical analysis revealed a significant decrease in TrkA levels compared to middle-aged female 3xTg-AD (**E**), whereas no changes in hippocampal TrkA levels were detected with age in male 3xTg-AD mice, but were significantly higher compared to middle-aged ntg mice (**F**). (*, $p<0.01$ and #, $p<0.05$, data was analyzed with a non-parametric Kruskal-Wallis test and Dunn's post hoc test for multiple comparisons). Abbreviations: ntg, non-transgenic mice; 3xTg, 3xTg-AD transgenic mice; error bars=standard error of the mean; mo, months.

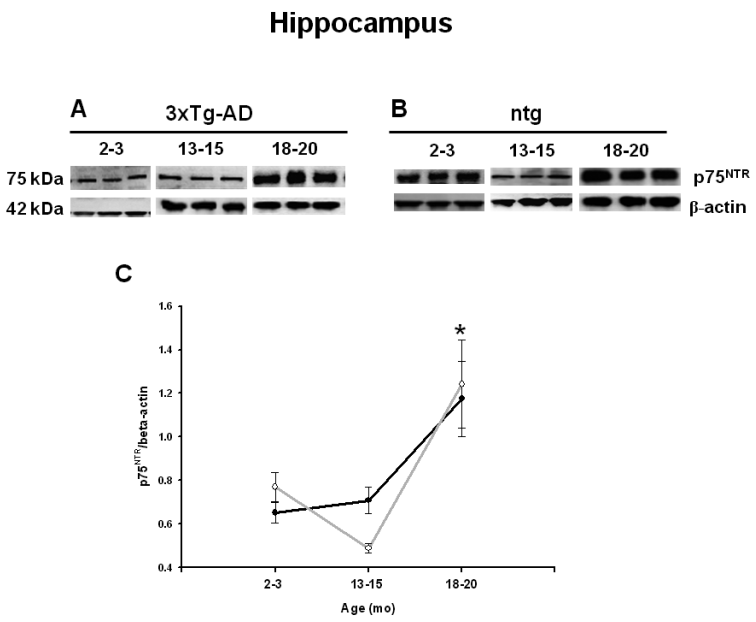

Figure 9.

A and **B**. Representative immunoblots from the hippocampus of 2 to 3, 13 to 15 and 18-20 month-old 3xTg-AD and ntg mice probed with antibodies against $p75^{NTR}$ and β-actin, respectively. **C**. Linear analysis of mean densitometry measurements from cortical $p75^{NTR}$-ir signals normalized to β-actin-ir in 3xTg-AD and ntg mice. Statistical analysis revealed a significant increased in $p75^{NTR}$ levels in aged 3xTg-AD mice compared to middle-aged mutant mice. (*, $p<0.01$, data was analyzed with a non-parametric Kruskal-Wallis test and Dunn's post hoc test for multiple comparisons). Abbreviations: ntg, non-transgenic mice; 3xTg, 3xTg-AD transgenic mice; error bars=standard error of the mean; mo, months.